Available online at www.sciencedirect.com
SCIENCE DIRECT
ELSEVIER
Journal of Molecular Catalysis A: Chemical 207 (2004) 183–193
JOURNAL OF MOLECULAR CATALYSIS A: CHEMICAL
www.elsevier.com/locate/molcata

Preparation, characterization and photocatalytic property of the $PW_{11}O_{39}^{7-}/TiO_2$ composite film towards azo-dye degradation

Danfeng Li [a], Yihang Guo [a], Changwen Hu [a,b,*], Chunjie Jiang [a], Enbo Wang [a]

[a] *Institute of Polyoxometalate Chemistry, Faculty of Chemistry, Northeast Normal University, Changchun 130024, PR China*
[b] *Department of Chemistry, Beijing Institute of Technology, Beijing 100081, PR China*

Received 3 April 2003; received in revised form 26 June 2003; accepted 27 June 2003

Abstract

The $PW_{11}O_{39}^{7-}/TiO_2$ (PW_{11}/TiO_2) composite film was prepared by $Ti(OC_4H_9)_4$ hydrolysis sol–gel method and a spin-coating technique for the first time. Physical measurements such as ultraviolet-visible (UV-Vis) spectroscopy, FT-infrared spectroscopy (FT-IR), ^{31}P MAS NMR, X-ray diffraction (XRD) and scanning electron microscopy (SEM) were employed to identify the structure and surface morphology of the film. The results reveal that the original Keggin structure of the PW_{11} remained intact on the film at the calcination temperature up to 350 °C, and the strong chemical interactions between the PW_{11} anion and TiO_2 matrix existed in the films. The photocatalytic activity of the PW_{11}/TiO_2 composite film calcined from 250 to 400 °C were tested via degradation of aqueous azo-dye, Congo Red (CR). It was observed that the film calcined at 350 °C had the highest photocatalytic activity, and the acidity of the system had an important effect on the photocatalytic process. In addition, comparing with the pure TiO_2 film and PW_{11}/SiO_2 composite film, the film showed remarkable photocatalytic activity, attributed to $PW_{11}O_{39}^{7-}$ catalyzed electron transfer from the conduction band (CB) of photoexicited TiO_2 to itself. The photocatalytic efficiency of the films had little change during several times of cyclic operation, indicating that the as-synthesized composite films were stable.
© 2003 Elsevier B.V. All rights reserved.

Keywords: Polyoxometalate (POM); Sol–gel; TiO_2 (anatase); Composite film; Photocatalysis; Congo Red (CR); Degradation

1. Introduction

The applications of TiO_2 or POMs (especially polyoxotungstates) for environmental protection and remediation have attracted much attention in recent years [1–7]. Now we have a fair degree of understanding of TiO_2 photocatalysis and POMs photocatalysis [8–10]. For TiO_2 photocatalyst, the photogeneration of highly reactive hole (h^+)–electron (e^-) pairs is the key effect for its photoactivity; while for polyoxotungstate catalysts, it is the formation of the O → W charge transfer (OWCT) excited state that plays a critical role. An apparent disadvantage of commonly used TiO_2 or POMs photocatalysis processes is the fact that they are difficult to be separated from the reaction systems, which impedes their ready recovery and reuse [11,12]. Therefore, from the standpoint of practical application, preparation of immobilized TiO_2 or POM composites may offer more practical benefits [13–21]. In a previous work, we have successfully synthesized XW_{11}/SiO_2 (X: Si, Ge and P) composite films through sol–gel method [22]. The films exhibited high photocatalytic activity towards formic acid degradation and high stabilities in the aqueous solution. Considering the fact that the SiO_2 matrix is not photoactive and hoping to improve further the photocatalytic activity of this type of the composite films, we synthesized POM/TiO_2 composite film in the present work for the first time. An important reason to replace SiO_2 by TiO_2 as the support is owing to the fact that the TiO_2 is also photoactive, thus the synergistic effect resulting from the combination of the starting POM and the TiO_2 support will increase the photocatalytic activity of either POM or TiO_2. Previous researches have shown that POMs can act as effective electron scavengers in the POM-containing TiO_2 systems during redox reactions while their structure remains intact [23–27]. Therefore, the recombination of h^+ and e^- was inhibited due to POM-catalyzed electron transfer from the CB of photoexcited TiO_2 to molecular oxygen, resulting in the photocatalytic activity of the system improved greatly. Purpose of selecting lacunary PW_{11} as the POM precursor

* Corresponding author. Tel.: +86-10-8257138; fax: +86-10-82571381.
E-mail address: huchw@nenu.edu.cn (C. Hu).

1381-1169/$ – see front matter © 2003 Elsevier B.V. All rights reserved.
doi:10.1016/S1381-1169(03)00491-6

is due to its strong reactivity towards the hydroxyl groups of titania (≡Ti–OH). As removal of a W–O octahedral moiety from a saturated polyoxotungstate framework leads to an increase and localization of the anionic charge, and the resulting lacunary anion becomes highly nucleophilic and reacts easily with electrophilic groups. After the ≡Ti–OH group was chemically grafted on the vacant site of PW_{11} anion, the surface of the PW_{11} anion would be saturated and the strong interaction between them ensured little lose of the PW_{11} anion from the film.

The PW_{11}/TiO_2 film was synthesized according to the following three steps. First, preparation of PW_{11}/TiO_2 sol via hydrolysis of $Ti(OC_4H_9)_4$ at pH 1.5 in the presence of PW_{11}; second, coating of the sol on a quartz slide by high-speed spinning; and third, calcination of the slide at 350 °C for 1 h. In the present work, degradation reaction of azo-dye Congo Red (CR) was used to test the photocatalytic activities of PW_{11}/TiO_2 composite films. As is well known, azo-dyes are a kind of colored organic pollutants that represent an increasing environmental danger [28]. CR is used extensively in a variety of coloration aspects. Besides the high photocatalytic activity of the PW_{11}/TiO_2 film, apparent advantage at reuse and recovery aspects can be shown, just as mentioned above. The aim of the present research is to create a new class of practicable photocatalytic film system based on photoactive TiO_2 and POM both, which was expected to have efficient photoactivity on azo-dye degradation.

2. Experimental

2.1. Materials and apparatus

$Na_7PW_{11}O_{39}$ was prepared according to a reference method [29]. $Ti(OC_4H_9)_4$, C_2H_5OH, EtOH, $NH_3{\cdot}H_2O$, H_2O_2, HCl, and CR were analytical regents. Doubly distilled water is used throughout the process. The chemical structure of azo-dye CR is presented in Fig. 1.

Ultraviolet-visible (UV-Vis) absorption spectra of CR solution and FT-IR spectra were recorded on a 756 CRT UV-Vis spectrophotometer and a Nicolet 205 FT-IR spectrometer, respectively. ^{31}P MAS NMR spectra were recorded on a Varian Unity-400 NMR spectrometer. SEM images were obtained on a Hitachi S-570 scanning electron microscope operating at 20 kV. Chemical compositions of the films were estimated by a Leeman Plasma SPEC (I) ICP–AES. Changes in the concentration of NH_4^+, SO_4^{2-}, NO_2^-, and NO_3^- were measured by a DX-300 ion chromatograph (IC) equipped with a COM-Π conductivity detector. CS12 cation column was used for determination of NH_4^+; AS4A anion column was used for determination of SO_4^{2-}, NO_2^-, NO_3^-; ICE–ASI anion column was used for determination of organic acid such as formic acid and acetic acid. Some of the intermediates during the degradation reaction were detected by LCQ electrospray mass spectrometer (ES–MS). Total organic carbon (TOC) concentrations of solutions were analyzed with a Tekmar, Dohrmann Apollo9000 TOC analyzer.

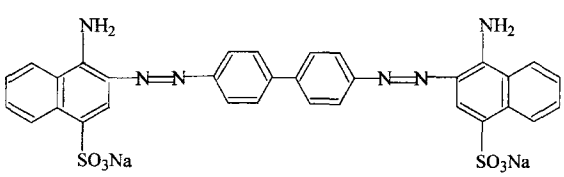

Fig. 1. Chemical structure of CR dye.

The quartz slides (1.25 mm × 12 mm × 45 mm) used for UV-Vis absorption measurements were cleaned (70 °C, 20 min) by immersion in a solution containing $NH_3{\cdot}H_2O$, H_2O_2 and H_2O with the volume ratio of 1:1:5, and then thoroughly washed with water.

2.2. Photoreactor and light source

The photoreactor was designed with a cylindrical quartz cell configuration and an internal light source surrounded by a quartz jacket, where aqueous CR solution completely surrounded the light source. Two slides of the films were placed near the wall of the reactor. An external cooling flow of water was used to maintain the reaction temperature constant. The optical pathlength was ca. 3 cm. The light source was a 125 W high-pressure mercury lamp (HPML, output mainly at 313.2 nm).

2.3. Catalyst preparation

The preparation of the PW_{11}/TiO_2 film catalyst was as follows. $Ti(OC_4H_9)_4$ (3 ml) was mixed with C_2H_5OH (12 ml), and the mixture was vigorously stirred; while stirring, the pH of the mixture was adjusted to 1.5 with HCl. After 5 min, an aqueous $Na_7PW_{11}O_{39}$ solution (0.05 M, 1 ml) was added dropwise. The above acidic mixture was continually stirred for 3 h until a homogenous sol was obtained. Then the sol was spin-coated on a quartz slide. The PW_{11}/TiO_2 film was finally synthesized by calcination of the slide at a temperature of 350 °C for 1 h. In order to investigate the effect of calcination temperature on the structure as well as the photoactivity of as-prepared films, other spin-coated films calcinated at different temperature (250 and 400 °C) were prepared. In addition, the PW_{11}/SiO_2 composite film and the pure TiO_2 film were synthesized with the same sol–gel method for comparison.

2.4. Photocatalytic procedure and analyses

Photodegradation of CR was carried out at atmospheric pressure using air as oxidant in the photoreactor. In a typical experiment, a 250 ml of CR solution (concentration: 0–30 mg/l) was placed in the photoreactor under vigorously stirring. Prior to irradiation, the film was immerged into the solution in dark for 30 min to ensure adsorption/desorption equilibrium. After the signal intensity of the HPML became stable, the solution was irradiated. In order to monitor the

dye concentration in the solution, a little amount of reaction solution (ca. 3 ml) for UV-spectroscopy analysis was taken from the photoreactor at appropriate time intervals.

3. Results and discussion

3.1. Characterization of the PW_{11}/TiO_2 film

Retention of the structural integrity of PW_{11} in the composite films was confirmed by UV-Vis, FT-IR, and ^{31}P MAS NMR. UV-Vis spectra of the starting PW_{11}, TiO_2, and the PW_{11}/TiO_2 films prepared at different calcination temperature are shown in Fig. 2. From Fig. 2, it can be seen clearly the characteristic absorption peaks at 202 and 257 nm of the starting PW_{11}, which were attributed to O → W charge transfer of the Keggin unit at W=O bond and W–O–W bond, respectively. However, the OWCT band at W–O–W bond changed from flat to sharp after formation of the PW_{11}/TiO_2 composite films (350 °C), and the OWCT band at W–O–W bond has a slightly red-shift from 257 nm (PW_{11}) to 268 nm (PW_{11}/TiO_2). The above result suggests that the Keggin structure of the PW_{11} anion tends to saturation in the synthesized films (350 °C). The saturation is owing to covalent bonding of the ≡Ti–OH groups from the titania network to the surface of the PW_{11} cluster via W–O–Ti bond. However, the characteristic peaks of PW_{11} cannot be seen for the PW_{11}/TiO_2 film (400 °C), therefore it can be concluded that the PW_{11} composite on the film is destroyed during the increase of temperature from 350 to 400 °C. The following XRD analyses may further evidence the conclusion. In addition, the observation of red-shift from 355 nm of the characteristic adsorption peak for TiO_2 to 386 nm that for the PW_{11}/TiO_2 film (350 °C) indicates that the interfacial action between TiO_2 matrix and PW_{11} existed on the film. Table 1 shows the characteristic IR fingerprints of

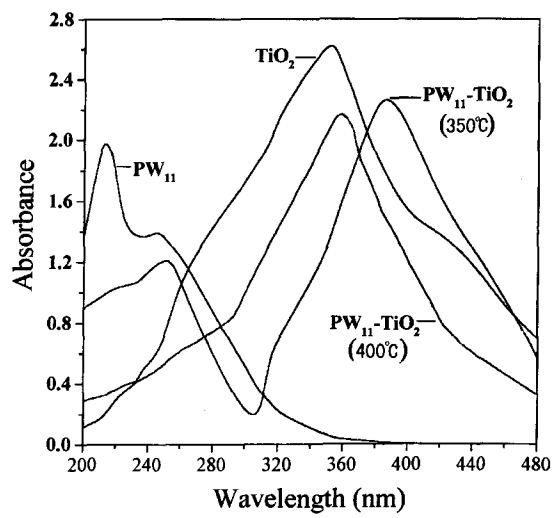

Fig. 2. UV absorbance spectra of the starting PW_{11} clusters, pure TiO_2 film and corresponding PW_{11}/TiO_2 films prepared at different calcination temperature (350 and 400 °C).

Table 1
Main relevant IR data (cm^{-1}) of the starting PW_{11} and their corresponding PW_{11}/TiO_2 (350 °C) films

Sample	ν as (P–O)	ν as (W=O)	ν as (W–O–W)
PW_{11}	1095, 1043	953	862, 833, 805, 730
PW_{11}/TiO_2 film[a]	1075, 1040	954	882, 818, 787, 692
PW_{11}/SiO_2 film	1079	953	870, 797, 672

[a] Vibration peak of Ti–O–W at 967 cm^{-1} in the composite film was observed.

PW_{11} in the region from ca. 1000 to 700 cm^{-1}, attributed to P–O bond in central PO_4 unit, W=O and W–O–W bond vibrations of PW_{11}, respectively [22]. In the case of pure PW_{11}, two IR vibration bands of P–O in central PO_4 were at 1095 and 1043 cm^{-1}, respectively; while in the PW_{11}/TiO_2 film (350 °C), the two vibration bands shifted to 1075 and 1040 cm^{-1}, respectively. The IR vibration bands may also arise from the P–O bond in central PO_4. Furthermore, it can be seen that the PW_{11}/TiO_2 films have other vibration bands similar to that of the starting PW_{11}, suggesting that the primary PW_{11} structures remained intact regardless of the functionality of the POM. The shifts of the positions of IR absorption peaks shown in the PW_{11}/TiO_2 films are due to the existence of covalent bonding between the surface oxygen atoms at the vacant sites of the PW_{11} and the titania matrix, similar to the interaction in the previously reported PW_{11}/SiO_2 film [22]. Integrant evidence in confirmation of the presence of the P–O bond from central PO_4 of PW_{11} in the PW_{11}/TiO_2 film (350 °C) is ^{31}P MAS NMR (Fig. 3). Resonance at δ −14.2 ppm, shown in Fig. 3, originated from the central PO_4 unit of PW_{11} cluster. According to the references reported ^{31}P MAS NMR data, chemical shift of the ^{31}P MAS NMR for pure PW_{12} and PW_{11}/SiO_2 were at δ −14.9 and −13.5 ppm, respectively; besides, the ^{31}P MAS NMR for pure PW_{11} and $PW_{11}TiO_{40}^{5-}$ were at δ −10.4 and −14.0 ppm [22,30,31]. The result of ^{31}P MAS NMR showed that the surface of the PW_{11} cluster tends to saturation after grafting of the ≡Ti–OH groups. The data is powerful in testifying the existence of chemical interaction between PW_{11} and titania matrix in the PW_{11}/TiO_2 composite film. Based on the above results, we can confirm that the structure of the PW_{11} remained intact after formation of the PW_{11}/TiO_2 composite film. Elemental analysis for the PW_{11}/TiO_2 com-

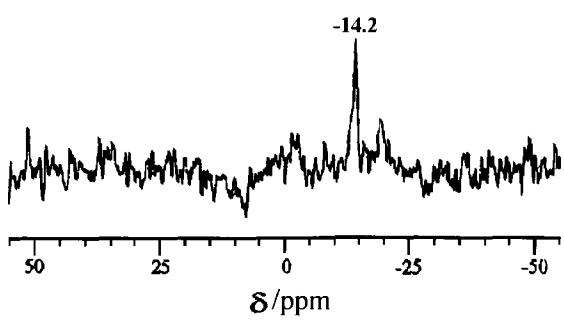

Fig. 3. ^{31}P MAS NMR spectrum of the PW_{11}/TiO_2 film (350 °C).

Table 2
Elemental analysis results, molar ratio (P:W), and the thickness of the PW_{11}/TiO_2 (350 °C), PW_{11}/SiO_2, and the pure TiO_2 film

Film	Na (%)	P (%)	W (%)	Ti (%)	Si (%)	Molar ratio (P:W)	The thickness of the film (nm)
PW_{11}/TiO_2	1.10	0.21	13.5	47.7		1:10.8	500
PW_{11}/SiO_2[a]	1.09	0.22	14.2		37.3	1:11.4	450
TiO_2[a]			60.6			400	

[a] PW_{11}/SiO_2 film and TiO_2 film were prepared under the similar condition with that of the PW_{11}/TiO_2 film.

posite film, the PW_{11}/SiO_2 composite film, and the pure TiO_2 film were shown in Table 2. It can be seen that the tungsten loadings for the two composite films are almost the same, suggesting that the photoactivity of the two composite films on the CR dye degradation are comparable. Determined molar ratio for P:W (close to 1:11) also confirmed retention of the Keggin structure of the PW_{11} in the film.

Fig. 4 shows the SEM images of the PW_{11}/TiO_2 film produced at different calcination temperature (250, 350, and 400 °C) for 1 h. The thickness of the film can be estimated from the edge of the visible crack, which is ca. 500 nm for the film calcined at 350 °C (see Table 2). It can be seen from the photos that the surface morphology of the film gradually becomes uniform from 250 to 350 °C. Appearance of large amount of holes and cracks at 400 °C indicated that the films were destroyed.

Fig. 5A–C illustrate the XRD patterns of the composite films calcined at 250, 350, and 400 °C, respectively. As can be easily detected from the XRD pattern of the composite film (250 °C), the crystallization of the film is close to amorphous. However, major peaks ($2\theta = 25.26$, 37.71, and 48.04°) showing the anatase phase was observed clearly as the calcination temperature increased to 350 °C. This occurred may be due to the crystallization of the films became more intense at the calcination temperature from 250 to 350 °C, and consequently reached maximum at 350 °C. In addition, comparing with the XRD pattern of the starting PW_{11} (Fig. 5D), the diffractions of the characteristics of pure PW_{11} phase can be easily seen in the films calcined at 350 °C (Fig. 5B). The existence of PW_{11} composite in the films is owing to the fact that PW_{11} is the inorganic precursor and remained intact under the experimental conditions.

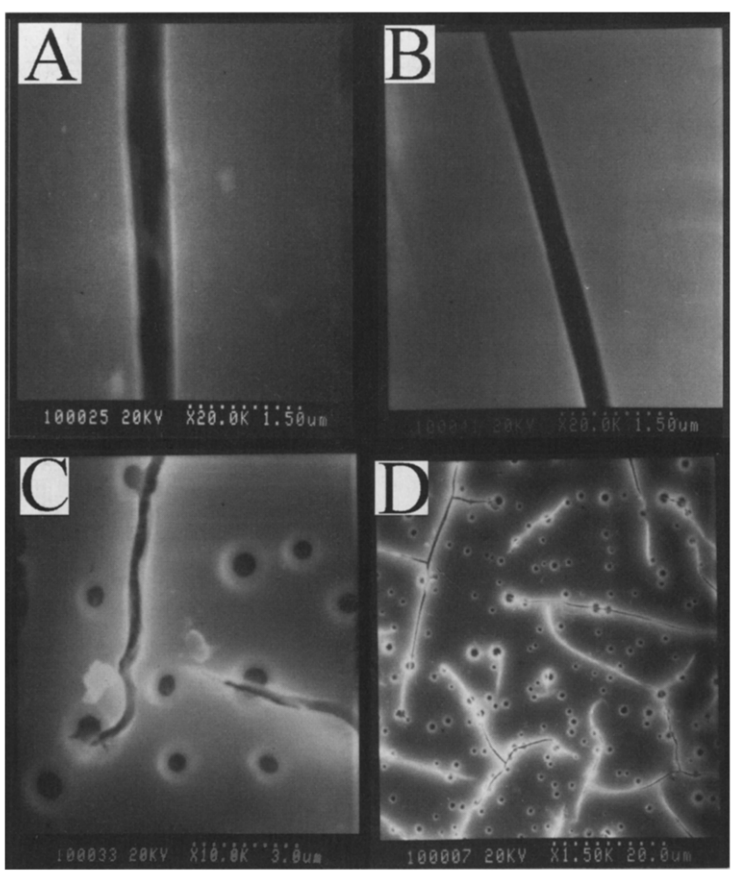

Fig. 4. SEM images of the PW_{11}/TiO_2 films. (A), (B), (C), and (D) are calcination temperature at 250, 350, 400 °C, respectively; (D) is the reduced image for (C).

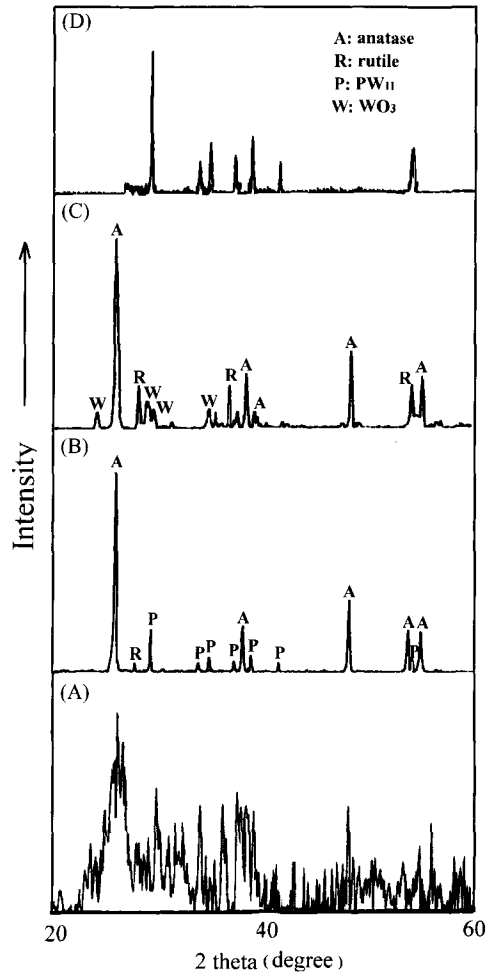

Fig. 5. XRD patterns for PW_{11}/TiO_2 films and original PW_{11}. (A), (B), and (C) for calcination temperatures 250, 350, 400 °C, respectively; (D) for the original PW_{11} composite.

On increasing the temperature to 400 °C, however, the intensities of the anatase peaks decreased while the intensities of the rutile peaks increased greatly. This revealed the occurrence of the anatase-rutile phase transformation in a large scale at the temperature range between 350 and 400 °C. Sharp decrease of the major peaks showing the PW_{11} phase and appearance of major peaks showing the tungsten oxide (WO_3) phase suggested that the PW_{11} is mostly decomposed to WO_3. The results are well in agreement with the SEM analyses discussed above. The phase transformation process is shown below.

newly spin-coated PW_{11}/TiO_2 film
↓ 250°C
PW_{11}/TiO_2 film (close to amorphous phase)
↓ 350°C
PW_{11}/TiO_2 film (TiO_2-anatase phase mainly)
↓ 400°C
WO_3+TiO_2 (TiO_2-rutile phase mainly)

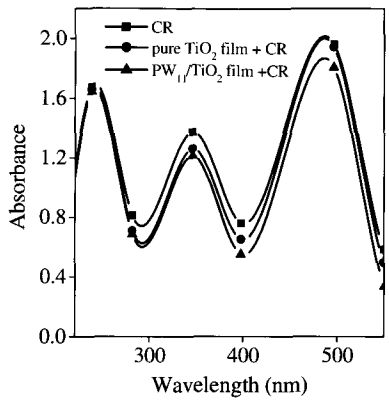

Fig. 6. Adsorption spectra of CR aqueous solution after adsorption for 12 h in the dark (C_0 = 30 mg/l, temperature at 25 °C): (■) blank, (●) TiO_2 film, (▲) PW_{11}/TiO_2 film.

3.2. Photocatalytic tests

3.2.1. Photocatalytic activity

Since the preadsorption of dyes before irradiation is very important for the photocatalysis process [32], the adsorption degree to CR dyes for the pure TiO_2 film and as-prepared film (calcined at 350 °C) were compared. As can be seen in Fig. 6, CR is much easier to be adsorbed on as-prepared films. From the results of absorbance at ca. 510 nm, it was estimated that about 7.8% of CR molecules were adsorbed on the former overnight; whereas only 0.9% of CR dyes were adsorbed on the pure TiO_2 films. The result indicated that the adsorbed amount of CR dye on the as-prepared films is ca. nine times that of the pure TiO_2 films, implying that the CR dye is easier to be adsorbed on the surface of the PW_{11}/TiO_2 film than that of the pure TiO_2 film. The reason may be relevant to the difference of the adsorption mode between the two types of films at the given acidity condition (pH = 5, unadjusted). As has been reported by Hu et. al., surface of the TiO_2/SiO_2 catalyst is negatively charged in the range of pH > 3, determined by Zeta-potential measurement [19,20]. Thus, it can be concluded that the anionic CR dye is difficult to be adsorbed on the surface of the TiO_2 film due to the repulsive electrostatic power between the negatively charged surface and the organic anion. However, for the PW_{11}/TiO_2 film, it was believed that the initial adsorption process is the ion-exchange between Na^+ existed in the PW_{11}/TiO_2 film and H^+ from the solution, thus protonization of the film in the solution occurred owing to the action of those H^+ with bridge O from W–O–Ti and W–O–W bond in the film. At the same time, $-NH_2$ groups from the CR dye were protonized to form $-NH_3^+$, and the sulfonate groups were adsorbed to the surface of the film via both electrostatic and hydrogen bonding interactions. Adsorption through sulfonate groups of dyes has already been confirmed in the case of indigo carmine dye photodegradation [8]. The overall adsorption process is shown in Scheme 1. Here, ellipsoid represents the main chain of the CR dye. This type of adsorption is an essential premise

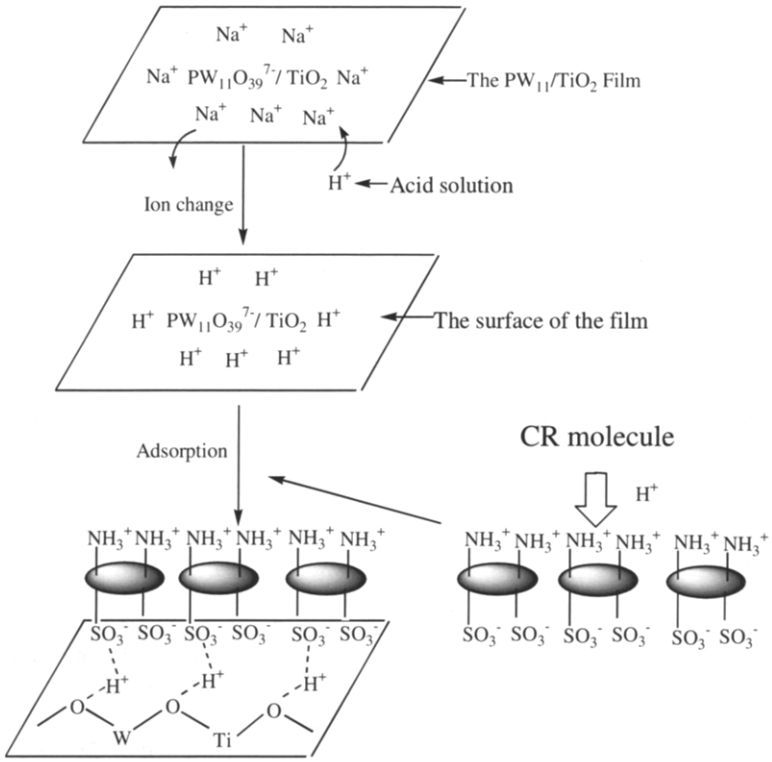

Scheme 1. Adsorption of CR dye on the PW_{11}/TiO_2 film.

for the heterogeneous photocatalytic degradation of the CR dye.

In order to confirm the note that the acidity of the solution is relevant to the adsorption of the sulfonate groups to the surface of the PW_{11}/TiO_2 films, effect of acidity on the heterogeneous photocatalytic oxidation of CR dye solution (30 mg/l) has been examined at pH from 3 to 11, and the results are presented in Fig. 7. It can be clear seen from the plot that the decolorization rate was slightly decrease from pH 3 to 5, suggesting the adsorption amount of sulfonate group on the film is almost the same at those acidities. However,

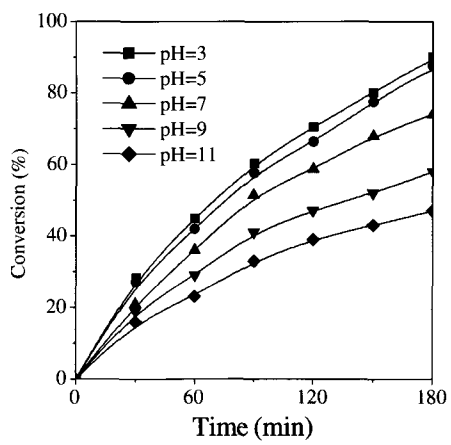

Fig. 7. Changes of conversion as a function of pH value of the solution under CR dye photodegradation reaction (the PW_{11}/TiO_2 film calcined at 350 °C is photocatalyst).

the value decreased significantly from pH 7 to 11, which may be ascribed to the change of chemisorptive abilities of sulfonate group to the PW_{11}/TiO_2 films. Since large amount of OH^- anions in the solutions will produce repulsive effect for the adsorption of sulfonate group, the photodegradation of the CR dye is inhibited accordingly.

The photocatalytic activities of as-prepared films at different calcinations temperature were tested via degradation of aqueous CR (30 mg/l) under near UV-irradiation, which are shown in Fig. 8. In the presence of those films, disappearance of CR is negligible in the dark. In the absence of the films, the changes of the concentrations of the CR solution are hardly observed under UV-irradiation (4 h). The above results indicate that the degradation of CR is mainly due to irradiation of the PW_{11}/TiO_2 films in the near UV area. As can be clearly seen from Fig. 8, the film calcined at 350 °C has the highest photoactivity among the three calcined PW_{11}/TiO_2 films. This result indicated that suitable calcination temperature for the PW_{11}/TiO_2 film is 350 °C. It may be relevant to the composition of the films calcined at different temperature, determined by XRD analyses. At lower calcination temperature (<350 °C), only a little amount of anatase phase in the film is formed. Therefore, the function of anatase, PW_{11}, and the electron transfer from anatase to PW_{11} cannot be well developed for the purpose of CR degradation. At higher calcination temperature (400 °C), since lots of the PW_{11} phase on the films was destroyed and transformed to WO_3 phase, which means that the function of POM as electron acceptor lost much; moreover, most of the anatase phase

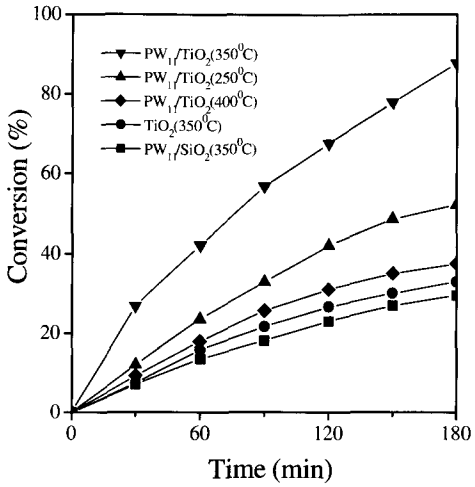

Fig. 8. Changes of conversion on the photodegradation of CR dye for the PW_{11}/TiO_2 films (calcination temperature 250, 350 and 400 °C, respectively), PW_{11}/SiO_2 film and pure TiO_2 film catalysts as a function of irradiation time.

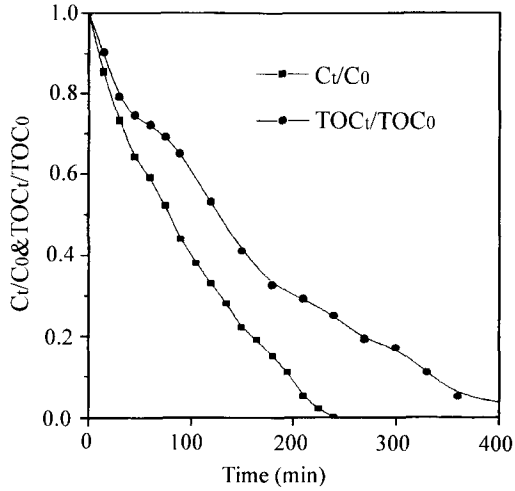

Fig. 9. Conversions of dyes and TOC removal with irradiation times for the CR dye solution (C_0: 30 mg/l, TOC_t and C_t refer to TOC and CR dye concentration of solution, respectively, at reaction time t, initial pH of the solution is 5; PW_{11}/TiO_2 film calcined at 350 °C as photocatalyst, temperature at 25 °C).

was transformed to rutile phase, the photocatalytic activity of the film decreased accordingly. The photocatalytic activity of the PW_{11}/TiO_2 film was also compared with those of the pure TiO_2 film and PW_{11}/SiO_2 composite film (Fig. 8). As for the pure TiO_2 film, only ca. 33% of CR disappeared under UV-irradiation for 180 min, while for the PW_{11}/SiO_2 film under the same degradation condition, it was found that the conversion (29.5%) is a little lower than that of the pure TiO_2 film. However, apparent decrease in the concentration of CR was observed by irradiating the CR solutions in the presence of the PW_{11}/TiO_2 film (350 °C), i.e. conversion of CR was ca. 88% till 180 min (almost 2.7 times that of the pure TiO_2 film). It can be concluded that the high photocatalytic activity of the PW_{11}/TiO_2 film (350 °C) arises from: (i) the existence of synergistic effect in the films during the photodegradation process, namely, recombination of h^+ and e^- was inhibited due to interfacial electron transfer from the CB of photoexcited TiO_2 to PW_{11}; (ii) intactness of the structure of the PW_{11}, which may involve in the photocatalytic cycle; (iii) TiO_2 composite at this temperature has the anatase phase mainly, which has better photoactivity than that of the rutile phase; and (iv) the difference of the adsorption ability of the PW_{11}/TiO_2 composite film and the pure TiO_2 film.

Fig. 9 shows the decolorization and overall TOC removal of CR dye solution. As shown, complete color removal needed up to around 250 min, while the complete removal of TOC of the reaction solution needed prolonged irradiation (ca. 400 min). Obviously, decolorization is easier than the TOC removal.

In order to observe the changes of the PW_{11}/TiO_2–CR reaction system in situ, the reaction was paused after UV-irradiation of the system for 40 min. It was found that the color of the film changed quickly from light blue to colorless, indicating the formation of the reduced form of PW_{11} heteropoly blue (HPB) due to accepting electrons from photoexcited TiO_2 during the reaction. The decoloration is due to the reoxidization of HPB by dioxygen in ambient environment.

According to the discussion above, the proposed process of photooxidation of CR is described below. First, precomplexion is carried out on the interface between the CR molecule adsorbed from the solution and the PW_{11}/TiO_2 on the film, which led to the formation of the charge transfer complex, $[PW_{11}/TiO_2{\cdot}CR]^{\#}$ (Eq. (1)),

$$PW_{11}/TiO_2 + CR \leftrightarrow [PW_{11}/TiO_2 \cdot CR]^{\#} \quad (1)$$

Second, UV-illumination of the $[PW_{11}/TiO_2{\cdot}CR]^{\#}$ to yield its excited state, and then formation of $OH^{\bullet}$ radicals with H_2O (Eqs. (2) and (3)),

$$[PW_{11}/TiO_2 \cdot CR]^{\#} + h\nu \rightarrow [PW_{11}/TiO_2 \cdot CR]^{\#*} \Leftrightarrow (h^+ + e^-)[PW_{11}/TiO_2 \cdot CR]^{\#} \quad (2)$$

$$h^+ + H_2O \rightarrow OH^{\bullet} + H^+ \quad (3)$$

In addition, when CR concentrations are higher than 200 mg/l, a different path may happen since the CR dye may react with the h^+ to form its radicals state, and then undergo oxidation reaction by molecular oxygen dissolved in solution, just as shown in Eq. (4), CR_{ox} included the final products as well as intermediate products of CR degradation reaction, which are determined by IC and ES–MS measurements.

$$CR + h^+ \rightarrow CR^{\bullet} \xrightarrow{O_2} CR_{ox} \quad (4)$$

The electrons yielded via Eq. (2) were attracted by PW_{11}, which was then reduced to its reduced form Eq. (5),

$$[PW_{11}/TiO_2 \cdot CR]^{\#} + e^- \rightarrow [PW_{11}/TiO_2]_{red} + CR \quad (5)$$

Here, the function of PW_{11} from $[PW_{11}/TiO_2{\cdot}CR]^{\#}$ is mainly as an electron acceptor, therefore, the recombination of h^+ and e^- was inhibited by its attraction of e^- from the CB of TiO_2.

Third, the photooxidation of the CR dye by $OH^\bullet$ in deep level (Eq. (6)),

$$CR + OH^\bullet \rightarrow CR_{ox} \quad (6)$$

The photoactivity of PW_{11} was decreased greatly due to the formation of HPB via attraction of e^- from the CB of TiO_2. Therefore, only a little amount of PW_{11} from $[PW_{11}/TiO_2{\cdot}CR]^{\#}$ will be photoexcited and involved in the CR degradation reaction, i.e. the photooxidation reaction from the $[PW_{11}/TiO_2{\cdot}CR]^{\#*}$ itself (Eq. (7)):

$$[PW_{11}/TiO_2 \cdot CR]^{\#*} \rightarrow [PW_{11}/TiO_2]_{red} + CR_{ox} \quad (7)$$

Fourth, reoxidation of $[PW_{11}/TiO_2]_{red}$ to its original oxidation state by dioxygen dissolved in the reaction system Eq. (8):

$$[PW_{11}/TiO_2]_{red} + H^+ + O_2 \rightarrow PW_{11}/TiO_2 + H_2O \quad (8)$$

After undergoing the above photocatalysis steps, a net photocatalytic cycle has been completed. The reoxidized form of PW_{11}/TiO_2 film was then capable of engaging in another series of electron transfers until CR was mineralized completely. Therefore, cycles of photooxidation of an aqueous CR dye over the PW_{11}/TiO_2 films were proposed and are shown in Scheme 2. In the present experiment, the concentration of CR is low, and the CR molecules are not strongly adsorbed on the surface of the film, therefore, it is impossible for the direct reaction of CR dye with holes to occur (Eq. (4)). For the purpose of clarity, this step was not appeared in the Scheme 2, although this path may happen when the concentrations of CR are higher than 200 mg/l.

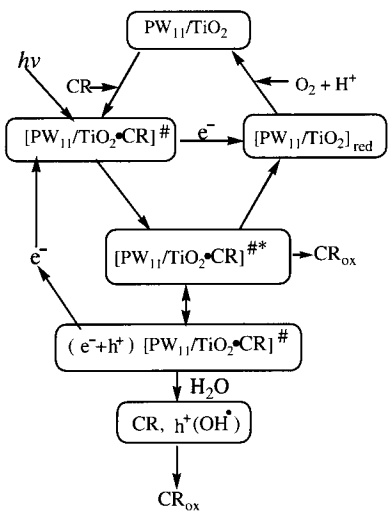

Scheme 2. Cycles of photooxidation of CR dye over the PW_{11}/TiO_2 film.

3.3. Kinetic study

Influences of initial CR dye concentrations (C_0) on the initial degradation rates of CR were performed by UV-irradiation of the PW_{11}/TiO_2–CR system for 250 min. When C_0 (initial concentration of CR) is changed in the range of 0–30 mg/l, a plot of R_0 (initial CR disappearance rate) versus C_0 exhibits a nearly straight line, and the linear correlation coefficients (R) are ca. 0.998 for the photocatalytic material (Fig. 11, left). The value of K (the adsorption equilibrium constant) and k (the reaction rate constant) calculated from the plot was 1.31×10^{-4} l/mg and 51.3 mg/l/min, respectively.

The above first-order linear relationship can be explained in a Langmuir–Hinshelwood model (Eq. (9)):

$$R = \frac{k K C}{1 + K C} \quad (9)$$

As for the dilute solution, $K C \ll 1$ because of the relatively weak adsorption of CR molecules on the surface of the film; therefore, the above model can be expressed by (Eq. (10)):

$$R_0 = k K C_0 \quad (10)$$

Therefore, the disappearance of CR follows a Langmuir–Hinshelwood first-order kinetic law for initial CR concentration chosen (0–30 mg/l).

3.4. Photocatalytic pathway of the CR dye

The intermediates and final products generated during the CR degradation process were analyzed both by ES–MS and IC measurements. Those intermediate products were identified by interpretation of their molecule ion peaks $[(M + H)/Z]$ (M is the molecular weight of the intermediates) in the mass spectra. According to these results, we proposed CR degradation pathway given in Scheme 3. Successive degradation of CR may occur via the following steps: (i) cleavage of C–S bond between the aromatic ring and the sulfonate groups by $OH^\bullet$ radicals attack; (ii) successive opening of the aromatic rings; (iii) –N=N– double-bond cleavage; (iv) cleavage of various C–N and C–C bonds of the chromophore group; and (v) decarboxylation by $OH^\bullet$ radicals based on Photo–Kolbe process:

$$RCOO^- + h^+ \rightarrow R^\bullet + CO_2 \quad (11)$$

3.5. Mineralization of CR dye

Evolutions of some intermediates such as acetic acid and formic acid, and inorganic products such as NH_4^+, SO_4^{2-}, NO_2^-, and NO_3^- as a function of irradiation time are shown in Fig. 10. It can be seen that the amount of the SO_4^{2-} and NO_3^- ions increased and gradually reached to a maximum as the irradiation time increasing, indicating that CR was mineralized totally. As for NH_4^+ and NO_2^- ions, however,

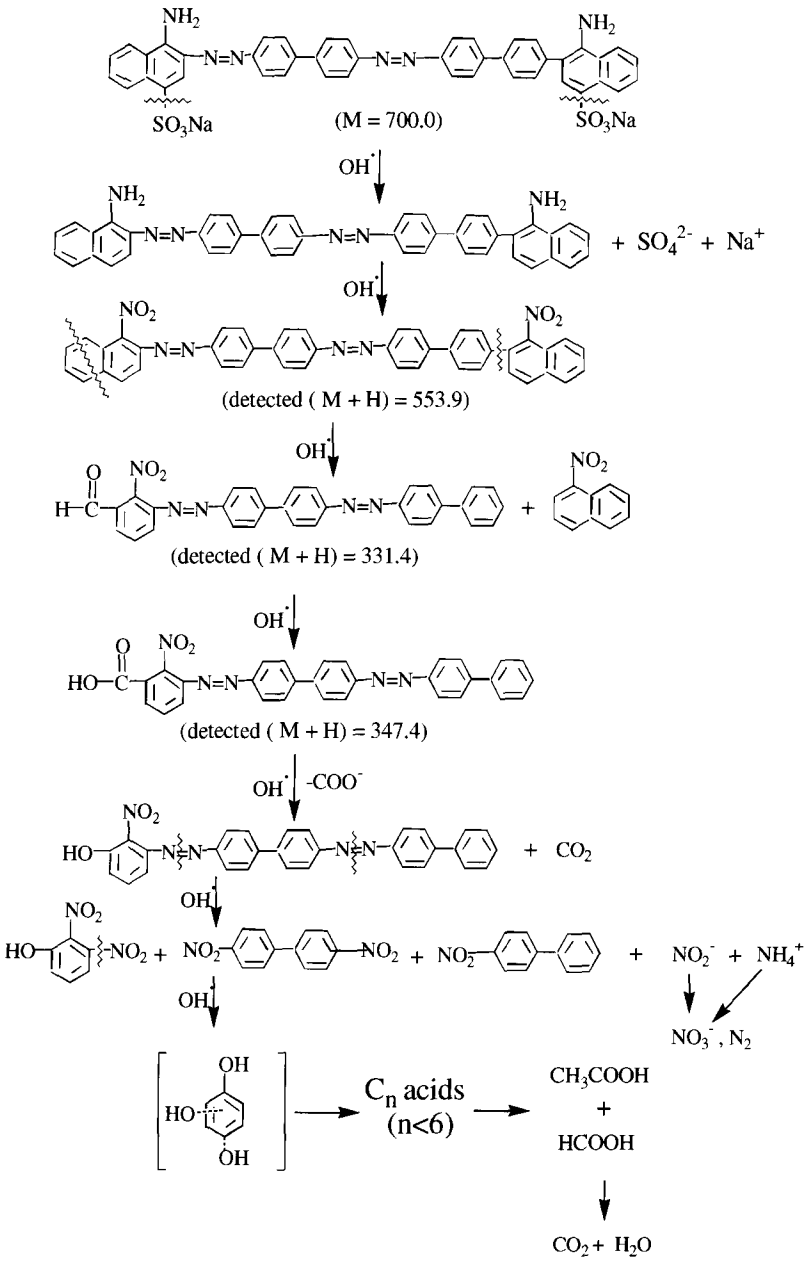

Scheme 3. Photodegradation pathway of CR in the presence of the PW_{11}/TiO_2 film.

both lines drops sharply at ca. 250 min while the formation rate of NO_3^- ion become faster at the same time. This result indicates that the transformation from NH_4^+ to NO_2^- or NO_3^- occurred. After ca. 400 min UV-irradiation, acetic acid disappeared, and then formic acid after another 50 min UV-irradiation, indicating that mineralization of CR into CO_2 was complete after ca. 450 min UV-irradiation in the presence of the composite films.

3.6. Recovery and lifetime of the PW_{11}/TiO_2 film catalysts

Having finished the first photocatalytic cycle, the absorbance of the PW_{11}/TiO_2 film (350 °C) was determined. The decrease of the absorbance values was hardly observed, indicating that the film was stable in aqueous CR dye solution. In addition, as is shown in Fig. 11 (right), the photoactivity of the PW_{11}/TiO_2 film was almost unchangeable after five catalytic cycles. It is apparent that the strong chemical interactions between the PW_{11} molecules and the titania matrix contribute to the result. At the same time, the tungsten contents of the reaction solution (PW_{11}/TiO_2–CR system) till the first photocatalytic cycle to the fifth were measured for 0.1, 0.07, 0.04, 0.03, and 0.02%, respectively, revealing that the drop of the PW_{11} from the film can be inhibited effectively. The above results suggest that the PW_{11}/TiO_2 film catalyst is suitable for the photodegradation reaction of aqueous CR dyes.

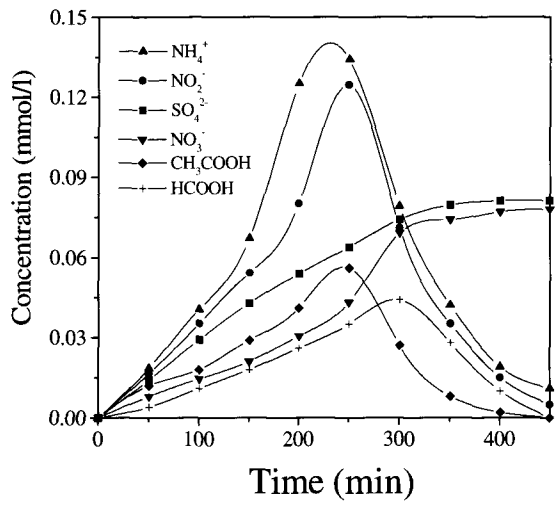

Fig. 10. Evolution of NH_4^+, SO_4^{2-}, NO_2^-, NO_3^-, acetic acid, and formic acid in solution during photocatalytic degradation of CR (C_0 = 0.043 mmol/l) on the PW_{11}/TiO_2 composite film.

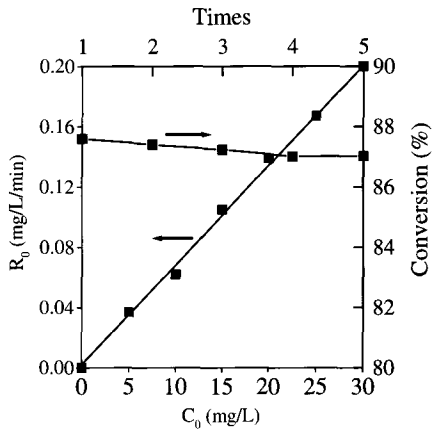

Fig. 11. Initial rate (R_0) vs. initial concentration (C_0) of photocatalytic degradation of CR (in the presence of the PW_{11}/TiO_2 film, C_0: 0–30 mg/l; temperature at 25 °C) (left). Lifetime of the PW_{11}/TiO_2 film calcined at 350 °C in the process of photocatalytic degradation of CR dye, C_0 = 30 mg/l, irradiating time 3 h as a function of reused times (right).

4. Conclusions

The PW_{11}/TiO_2 composite film was prepared via a simple sol–gel method for the first time. The primary Keggin structure of $PW_{11}O_{39}^{7-}$ cluster remained intact after formation of the composite film, and chemical interactions between $PW_{11}O_{39}^{7-}$ and TiO_2 via covalent bonding existed in the composite film. The original lacunary Keggin structure tended to saturation due to chemical fixation of the titania group to the surface of $PW_{11}O_{39}^{7-}$. The suitable calcination temperature for the PW_{11}/TiO_2 film is 350 °C based on the UV-Vis spectra, XRD analyses, and SEM results. The PW_{11}/TiO_2 film (350 °C) exhibits much higher photoactivity than that of pure TiO_2 film and PW_{11}/TiO_2 film towards CR dye degradation reaction under UV-irradiation. This high photoactivity of the PW_{11}/TiO_2 film is mainly due to $PW_{11}O_{39}^{7-}$ catalyzed electron transfer from the CB of photoexicited TiO_2 to itself. The disappearance of CR follows a Langmuir–Hinshelwood first-order kinetic law for initial CR concentration chosen (0–30 mg/l) by using the PW_{11}/TiO_2 composite film as photocatalyst. In addition, recovery and lifetime tests show that the composite films are stable and easily handled for recycling uses. The studies suggest that the PW_{11}/TiO_2 composite film has great potential for practical photodegradation applications.

Acknowledgements

The Natural Science Fund Council of China is acknowledged for financial support (nos. 20071007 and 20271007).

References

[1] C.S. Turchi, D.F. Ollis, J. Catal. 122 (1990) 178.
[2] A. Mylonas, E. Papaconstantinou, J. Mol. Catal. 92 (1994) 261.
[3] U. Stafford, K.A. Gray, P.V. Kamat, J. Catal. 167 (1997) 25.
[4] C. Hu, B. Yue, T. Yamase, Appl. Catal. A 194 (2000) 99.
[5] T. Okuhara, H. Watanabe, T. Nishimura, K. Lnumaru, M. Misono, Chem. Mater. 12 (2000) 2230.
[6] M. Misono, Chem. Commun. 13 (2001) 1141.
[7] T. Okuhara, Chem. Rev. 102 (2002) 3641.
[8] M. Vautier, C. Guillard, J.-M. Herrmann, J. Catal. 201 (2001) 46.
[9] S. Ahmed, T.J. Kemp, P.R. Unwin, J. Photochem. Photobiol. A: Chem. 141 (2001) 69.
[10] Y. Guo, C. Hu, S. Jiang, C. Guo, Y. Yang, E. Wang, Appl. Catal. B 36 (2002) 9.
[11] M.R. Hoffmann, S.T. Martin, W. Choi, D.W. Bahnemann, Chem. Rev. 95 (1995) 69.
[12] A. Molinari, R. Amadelli, V. Carassiti, A. Maldotti, Eur. J. Inorg. Chem. (2000) 91.
[13] A. Yasumori, K. Ishizu, S. Hayashi, K. Okada, J. Mater. Chem. 8 (1998) 2521.
[14] A. Molinari, R. Amadelli, L. Andreotti, A. Maldotti, J. Chem. Soc., Dalton Trans. (1999) 1203.
[15] Y. Guo, Y. Wang, C. Hu, Y. Wang, E. Wang, Chem. Mater. 11 (2000) 3501.
[16] C.R. Mayer, I. Fournier, R. Thouvenot, Inorg. Chem. Eur. J. 6 (2000) 105.
[17] Y. Guo, D. Li, C. Hu, Y. Wang, E. Wang, Y. Zhou, S. Feng, Appl. Catal. B 30 (2001) 337.
[18] A. Yasumori, H. Shinoda, Y. Kameshima, S. Hayashi, K. Okada, J. Mater. Chem. 11 (2001) 1253.
[19] C. Hu, Y. Wang, H. Tang, Appl. Catal. B 30 (2001) 277.
[20] C. Hu, Y. Wang, H. Tang, Appl. Catal. B 35 (2001) 95.
[21] I.M. Arabatzis, S. Antonaraki, T. Stergiopoulos, A. Hiskia, E. Papaconstantinou, M.C. Bernard, P. Falaras, J. Photochem. Photobiol. A: Chem. 149 (2002) 237.
[22] D. Li, Y. Guo, C. Hu, Y. Wang, L. Mao, E. Wang, Appl. Catal. A 235 (2002) 11.
[23] R.R. Ozer, J.L. Ferry, Environ. Sci. Technol. 35 (2001) 3242.
[24] T. Yamase, T. Usami, J. Chem. Soc., Dalton. Trans. (1988) 183.
[25] R.C. Chambers, C.L. Hill, J. Am. Chem. Soc. 112 (1990) 8427.

[26] H. Einaga, M. Misono, Bull. Chem. Soc. Jpn. 70 (1997) 1551.
[27] P. Gomez-Romero, Solid State Ionics 101 (1997) 243.
[28] H.M. Martin, Photodegradation of Water Pollutant, CRC Press, Boca Raton, 1996.
[29] N. Haraguchi, Y. Okaue, T. Isobe, Y. Matsuda, Inorg. Chem. 33 (1994) 1015.
[30] E. Wang, C. Hu, L. Xu, in: H. Liang (Ed.), Introduction of the Polyoxometalate Chemistry, Chemical Industry Press, Beijing, 1997, pp. 17, 40 (in Chinese).
[31] W.H. Knoth, P.J. Domaille, D.C. Roe, Inorg. Chem. 22 (1983) 198.
[32] Y. Ma, J. Yao, J. Photochem. Photobiol. A: Chem. 116 (1998) 167.